

## Supporting Information

### **Solid state characterization of oxidized actinides co-crystallized with uranyl nitrate hexahydrate**

Jeffrey D. Einkauff<sup>a</sup> and Jonathan D. Burns<sup>\*b</sup>

<sup>a</sup> Center for Nuclear Security Science & Policy Initiatives, Texas A&M University, College Station, TX 77843, USA

<sup>b</sup> Nuclear Engineering and Science Center, Texas A&M University, College Station, TX 77843, USA

\*To whom correspondence should be addressed.

E-mail: burns.jon@tamu.edu

## Materials

Nitric acid (69–70% Omni Trace,  $\text{HNO}_3$ ) was purchased from EDM; sodium bismuthate (ACS Grade,  $\text{NaBiO}_3$ ) was purchased from Alfa Aesar; uranyl nitrate hexahydrate (99+%,  $\text{UO}_2(\text{NO}_3)_2 \cdot 6\text{H}_2\text{O}$ ) was purchased from Strem Chemicals and all were used as received. Deionized (DI)  $\text{H}_2\text{O}$  was obtained from an ELGA LabWater Purelab Flex ultrapure laboratory water purification system operated at  $18.2 \text{ M}\Omega \text{ cm}$  at  $25 \text{ }^\circ\text{C}$ . Neptunium-237 oxide ( $\geq 99.99\%$ ,  $^{237}\text{NpO}_2$ ), plutonium-239 oxide ( $\geq 99.92\%$ ,  $^{239}\text{PuO}_2$ ), and americium-243 oxide ( $\geq 99.98\%$ ,  $^{243}\text{AmO}_2$ ), were purchased from the U.S. Department of Energy's National Isotope Development Center and were each converted to the nitrate form by dissolving in nitric acid under moderate heating ( $\sim 60\text{--}90 \text{ }^\circ\text{C}$ ). **WARNING:**  $^{237}\text{Np}$ ,  $^{239}\text{Pu}$ , and  $^{243}\text{Am}$  are all highly radioactive and were handled under ALARA principles in laboratories equipped to handle radioactive materials appropriately. Radiological fume hoods and glove boxes were employed.

The oxidation state and concentrations of the actinides in solution were determined by observing the optical spectra using an Ocean Optics QEPro UV–vis spectrometer and Ocean Optics Flame-NIR NIR spectrometer, an Ocean Optics HL-2000 halogen light source, and a path length of 1 cm. The data were obtained with OceanView analysis software from Ocean Optics and baseline-corrected with OriginPro 2018 Software. The concentration of the  $\text{UO}_2^{2+}$  was calculated by implementing Beer's Law with the molar extinction coefficient ( $\epsilon$ ) of  $5.47 \text{ L mol}^{-1} \text{ cm}^{-1}$  at 415 nm (see Fig. S3). The concentration of the  $\text{NpO}_2^{2+}$  was calculated with an  $\epsilon$  of  $41 \text{ L mol}^{-1} \text{ cm}^{-1}$  at 1221 nm (see Fig. S4). The concentration of the  $\text{PuO}_2^{2+}$  was calculated with an  $\epsilon$  of  $450 \text{ L mol}^{-1} \text{ cm}^{-1}$  at 830 nm (see Fig. S5). The concentration of the  $\text{Am}^{3+}$  was calculated with an  $\epsilon$  of  $251 \text{ L mol}^{-1} \text{ cm}^{-1}$  at 503 nm (see Fig. S6). The concentration of the  $\text{AmO}_2^+$  was calculated with an  $\epsilon$  of  $70 \text{ L mol}^{-1} \text{ cm}^{-1}$  at 717 nm (see Fig. S6). The concentration of the  $\text{AmO}_2^{2+}$  was calculated with an  $\epsilon$  of  $76.7 \text{ L mol}^{-1} \text{ cm}^{-1}$  at 996 nm (see Fig. S6). The concentration of the  $\text{NpO}_2^+$  was calculated by with an  $\epsilon$  of  $372 \text{ L mol}^{-1} \text{ cm}^{-1}$  at 980 nm (see Fig. S7). Quantitative analysis was performed via gamma ( $\gamma$ )-ray spectroscopy using a calibrated Canberra Model GC4018 high-purity germanium detector (HPGe) with an active detector volume of  $\sim 45 \text{ cm}^3$  and Lynx™ digital signal analyzer (DSA, Canberra Industries Inc., Meriden, CT). The detector has an energy resolution of 0.925 keV at 122 keV and 1.8 keV at 1300 keV. Relevant nuclear data were obtained from Browne and Firestone.<sup>1</sup> All calibrations were determined with a  $^{152}\text{Eu}$  standard  $\gamma$ -ray sources traceable to the National Institute of Standards and Technology (NIST) purchased from Eckert & Ziegler Isotope Products. The  $^{237}\text{Np}$  was tracked by using the 86.5 keV and 143 keV  $\gamma$ -rays. The  $^{243}\text{Am}$  was tracked by using the 43.5 keV and 142 keV  $\gamma$ -rays. The  $^{239}\text{Pu}$  was tracked semi-quantitatively by using the 59.5 keV  $\gamma$ -ray from  $^{241}\text{Am}$ , a decay daughter of the minor isotope  $^{241}\text{Pu}$  (0.012% w/w  $^{41}\text{Pu}/^{239}\text{Pu}$ ).

Scanning electron microscopy (SEM) using a JEOL 6400 Scanning Electron Microscope housed in the Fuel Cycle and Materials Laboratory (FCML) at Texas A&M University. The SEM electron beam was operated at 20 keV, and the images recorded the back-scattered electron (BSE) detector signal. Energy dispersive X-Ray Spectroscopy (EDS) was performed with the electron beam operating at 20 keV. All samples were carbon coated prior to imaging to prevent charging of the particles and improve image quality. The SEM and EDS X-ray maps are shown in Fig. S8, Fig. S9, Fig. S10, and Fig. S11. It should be noted, during the process of attempting to ensure the crystallites were adhered to the carbon tape used secure the samples during analysis, the crystallites containing  $\text{PuO}_2^{2+}$  and  $\text{AmO}_2^{2+}$ , and to a lesser extent  $\text{NpO}_2^{2+}$ , fractured and crumbled. While the

crumbled samples are not useful for determining the size or morphology of product, they do allow some insight to be gained from the interior of the crystallite, revealing uniform distribution of U and TRUs throughout the samples.

## Experimental

The general procedure for generating these samples was to first dissolve roughly 100 mg of uranyl nitrate (UN) solid in HNO<sub>3</sub> at approximately 50–60 °C in a water jacketed sand bath, which was temperature-controlled by a VWR® Refrigerated Circulating Baths Model 1166D with a VWR digital temperature controller, once all of the UN solid dissolved (after *ca.* 4 h of heating), the system was allowed to cool naturally to ambient temperature (~25 °C), during which crystallization occurred slowly (*cf.* Fig. S1). Table S1 summarizes the experimental conditions for each co-crystallization, with gamma spectroscopy results in Table S2, Table S3, Table S4, and Table S5. Once cooled, the solid and liquid phases were separated by centrifugation with a Costar® Spin-X® 0.45 µm cellulose acetate centrifuge tube filter with a mini-centrifuge. When the samples contained hexavalent transuranic (TRU) species, Np(VI), Pu(VI), or Am(VI), 3–4 mg of NaBiO<sub>3</sub> was added to the UN solid prior to the dissolution to ensure the hexavalent state was maintained throughout the crystallization process. An aliquot of the TRUs was then added to the UNH-NaBiO<sub>3</sub> mixture, which contained ~1–2.5 mg of the An(VI) species, dissolved in HNO<sub>3</sub>. For experiments involving Am(VI), only glass containers, pipettes, and cuvettes were used, as Am(VI) is a very strong oxidant and will react readily with available organic reductants; this includes plastic surfaces. In these cases, decantation was used rather than centrifugation to separate the phases. When the samples contain pentavalent TRU species, Np(V), the UNH was dissolved with an aliquot containing ~1.5 mg of Np(V) present, dissolved in 0.1 M HNO<sub>3</sub>. Optical spectra of the solution before and after crystallization were obtained, and the separated phases were analyzed by γ-ray spectroscopy.

Table S1: Experimental conditions for the co-crystallizations.

TRU Species	V <sub>15.8 M HNO<sub>3</sub></sub> (µL)	V <sub>H<sub>2</sub>O</sub> (µL)	V <sub>58°C</sub> (µL)	[HNO <sub>3</sub> ] <sub>58°C</sub> (M)	U (mg)	<sup>237</sup> Np (mg)	<sup>239</sup> Pu (mg)	<sup>243</sup> Am (mg)
Blank	2.00	58.0	91.1	0.35	37.6	-	-	-
Np(IV)	5.34	15.7	61.9	1.4	33.5	2.5 (2.2)	-	-
Pu(VI)	16.7	16.3	42.2	6.3	21.7	-	1.1 (1.1)	-
Am(VI)	20.4	20.4	114	2.8	75.3	-	-	1.0 (1.2)
Np(V)	0.13	20.8	44.0	0.047	32.1	1.5 (1.4)	-	-

Table S2: Gamma spectroscopy results of co-crystallization of UNH with NpO<sub>2</sub><sup>2+</sup> present.

ID	Live time (s)	86.5 keV (cps)	143 keV (cps)	Dead Time (%)	Distance (cm)
ML 60°C*	3600.0	33.2	1.49	0.84	1.15
ML 25°C**	529.9	23.9	1.18	2.34	1.15
Crystal Fraction 1	835.9	406	14.8	5.09	1.15
Crystal Fraction 2	602.6	43.4	1.79	2.39	1.15

\*1.75 µL aliquot of mother liquor

\*\*3.70 µL aliquot of mother liquor

Table S3: Gamma spectroscopy results of co-crystallization of UNH with  $\text{PuO}_2^{2+}$  present.

ID	Live time (s)	59.5 keV (cps)	Dead Time (%)	Distance (cm)
ML 60°C*	310.2	1040	5.07	1.15
ML 25°C**	324.2	1170	5.43	1.15
Crystal Fraction 1	3508.5	81.2	0.52	1.15
Crystal Fraction 2	3432.2	34.4	0.25	1.15
Crystal Fraction 3	-	-	-	-

\*5  $\mu\text{L}$  aliquot of mother liquor

\*\*10  $\mu\text{L}$  aliquot of mother liquor

Table S4: Gamma spectroscopy results of co-crystallization of UNH with  $\text{AmO}_2^{2+}$  present.

ID	Live time (s)	43.5 keV (cps)	142 keV (cps)	Dead Time (%)	Distance (cm)
ML 60°C*	300.0	5.93	1.37	7.77	23
ML 25°C**	300.0	3.9	1.13	7.83	23
Crystal Fraction 1	300.0	4.4	2.0	10.8	23
Crystal Fraction 2	1618.3	0.5	0.5	2.2	1001
Crystal Fraction 3	3600.0	0.2	0.1	0.8	1001
Crystal Fraction 4	2540.4	1.62	0.592	3.44	1001

\*5.25  $\mu\text{L}$  aliquot of mother liquor

\*\*4.95  $\mu\text{L}$  aliquot of mother liquor

Table S5: Gamma spectroscopy results of co-crystallization of UNH with  $\text{NpO}_2^+$  present.

ID	Live time (s)	86.5 keV (cps)	143 keV (cps)	Dead Time (%)	Distance (cm)
ML 60°C*	2203.9	12.1	0.331	0.49	23
ML 25°C**	2534.4	1.55	0.0514	0.08	23
Crystal Fraction 1	2632.9	10.4	0.352	0.19	23
Crystal Fraction 2	602.6	43.4	1.79	2.39	1.15
Crystal Fraction 3	994.2	40.4	1.61	1.9	1.15

\*2  $\mu\text{L}$  aliquot of mother liquor

\*\*2  $\mu\text{L}$  aliquot of mother liquor

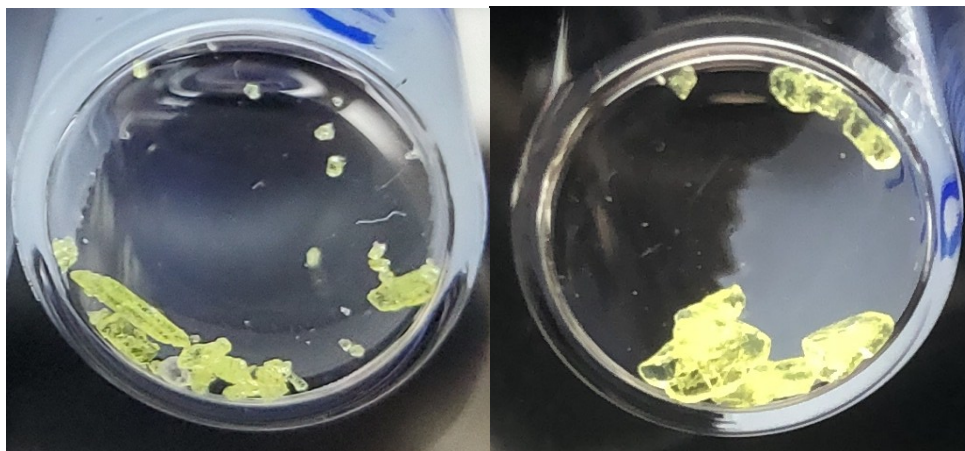


Fig. S1 Crystalline product resulting from the co-crystallization of  $\text{AmO}_2^{2+}$  (left) and  $\text{NpO}_2^+$  (right) with UNH.

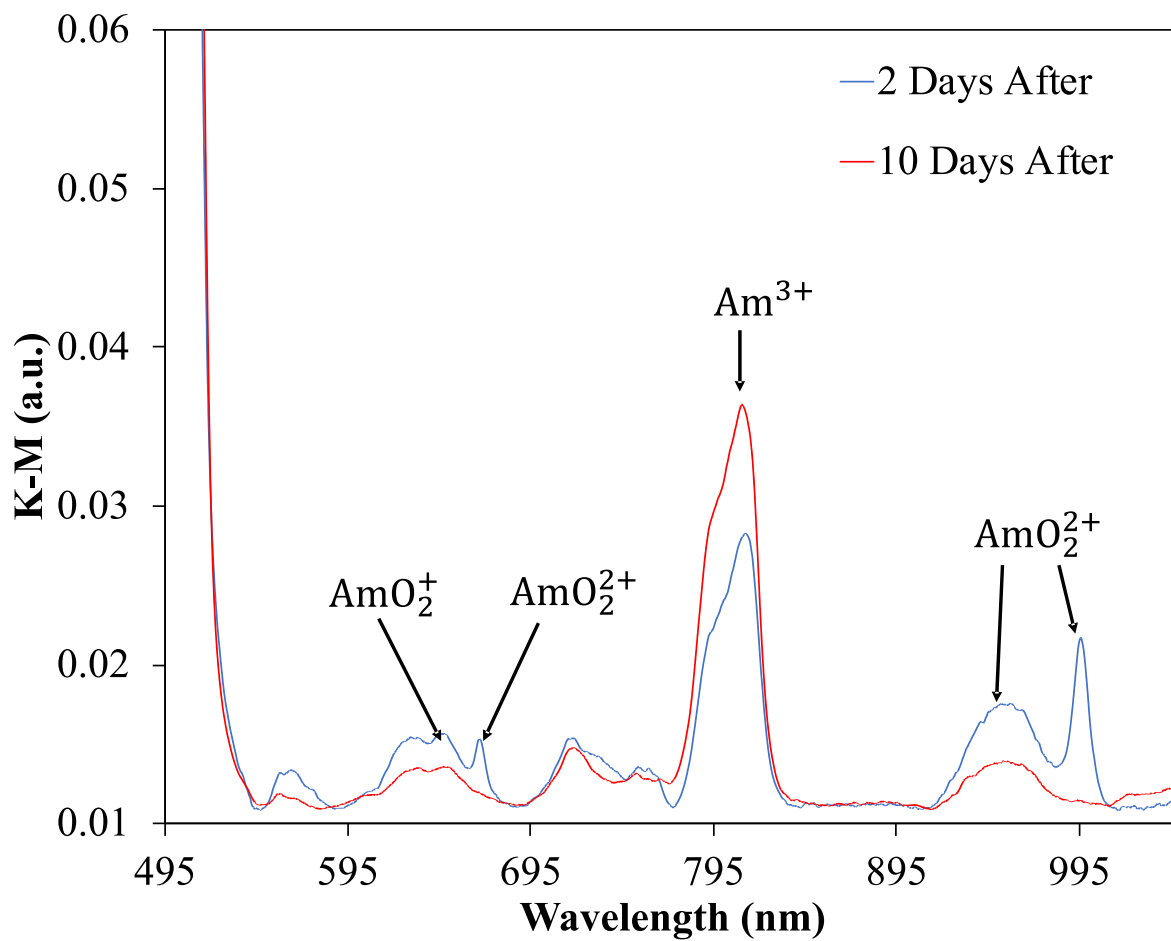


Fig. S2 Kubelka-Munk function 2 d (blue) and 10 d (red) after crystallization of the UNH with  $\text{AmO}_2^{2+}$ .

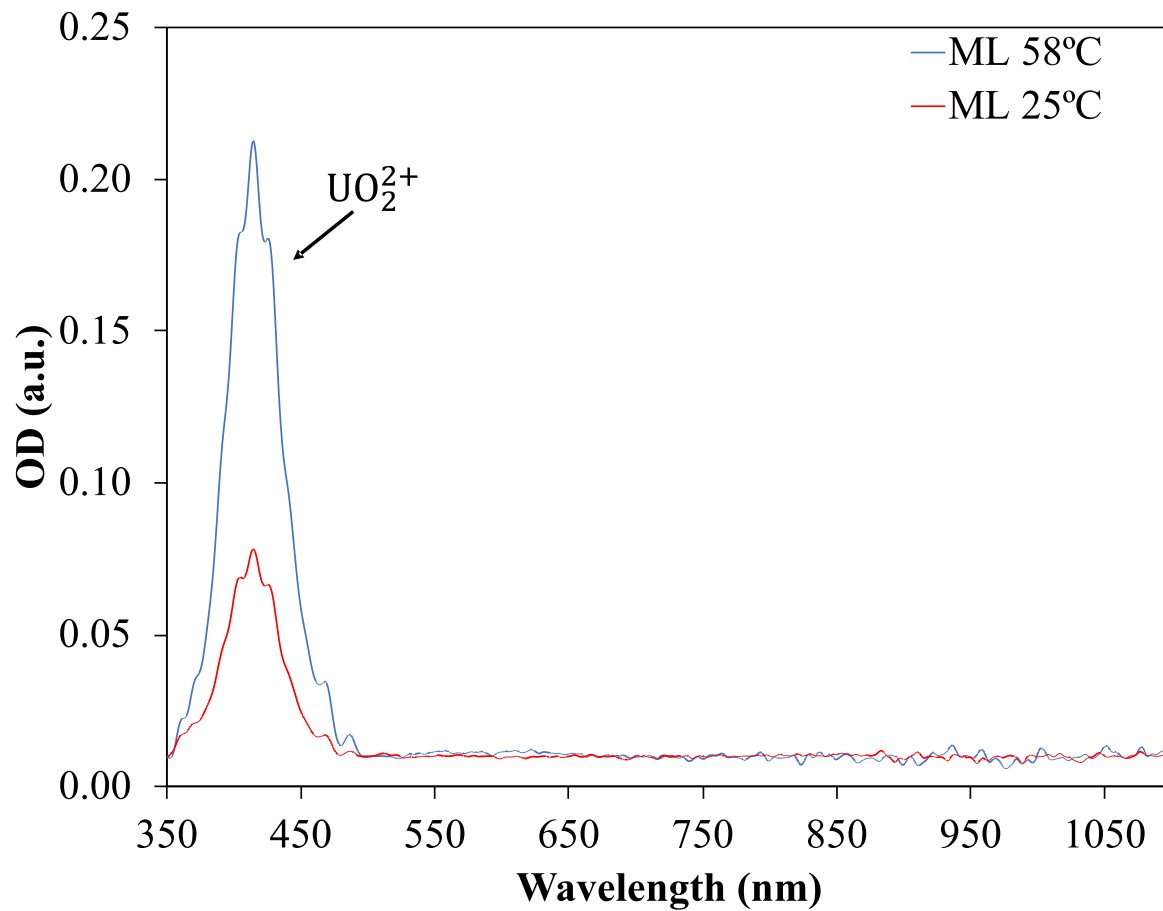


Fig. S3 Spectra of co-crystallization of UNH before (blue) and after (red) crystallization diluted 50-fold.

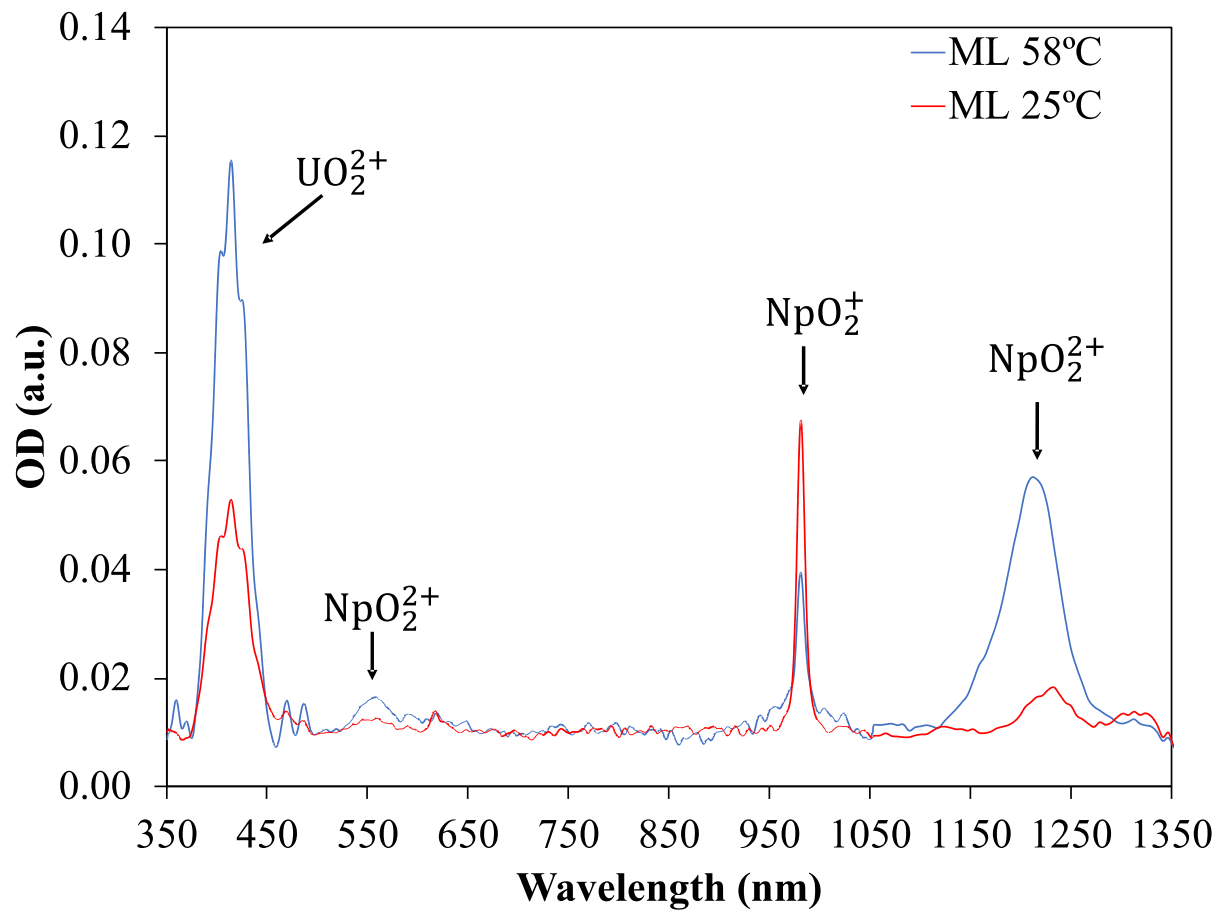


Fig. S4 Spectra of co-crystallization of UNH with  $\text{NpO}_2^{2+}$  present before (blue) and after (red) crystallization diluted 115 and 55-fold, respectively.

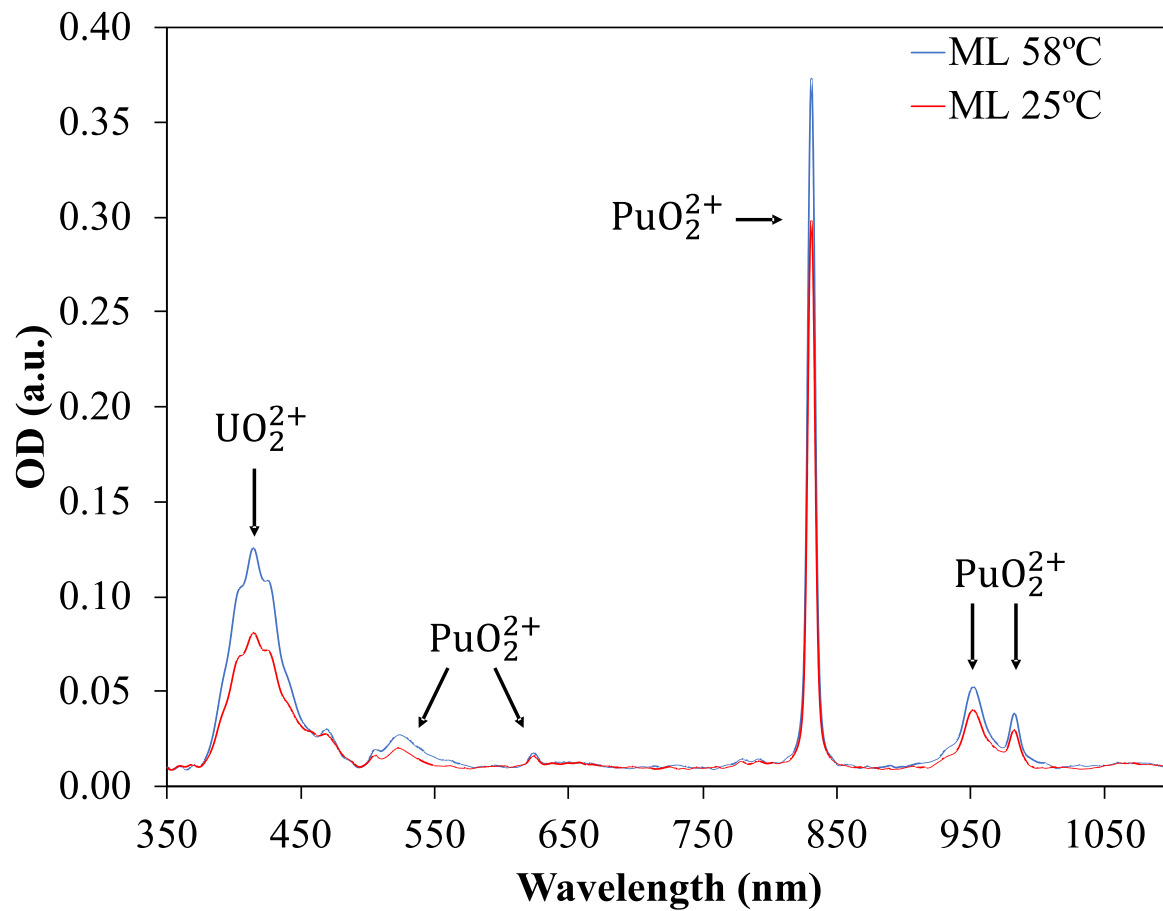


Fig. S5 Spectra of co-crystallization of UNH with PuO<sub>2</sub><sup>2+</sup> present before (blue) and after (red) crystallization diluted 100 and 50-fold, respectively.



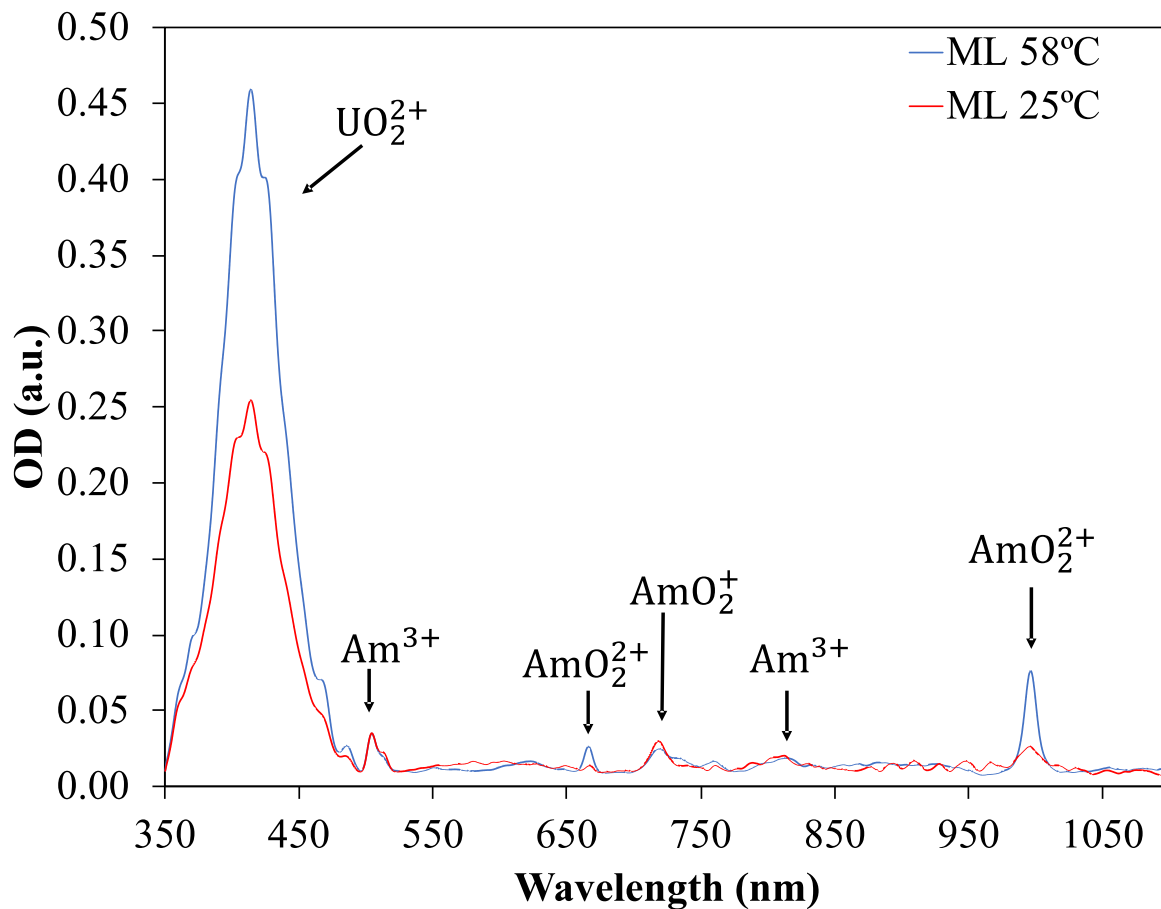


Fig. S6 Spectra of co-crystallization of UNH with  $\text{AmO}_2^{2+}$  present before (blue) and after (red) crystallization diluted 39 and 41-fold, respectively. It should be noted, all three of the stable oxidation states  $\text{Am}^{3+}$  (10%),  $\text{AmO}_2^+$  (12%), and  $\text{AmO}_2^{2+}$  (78%) present.

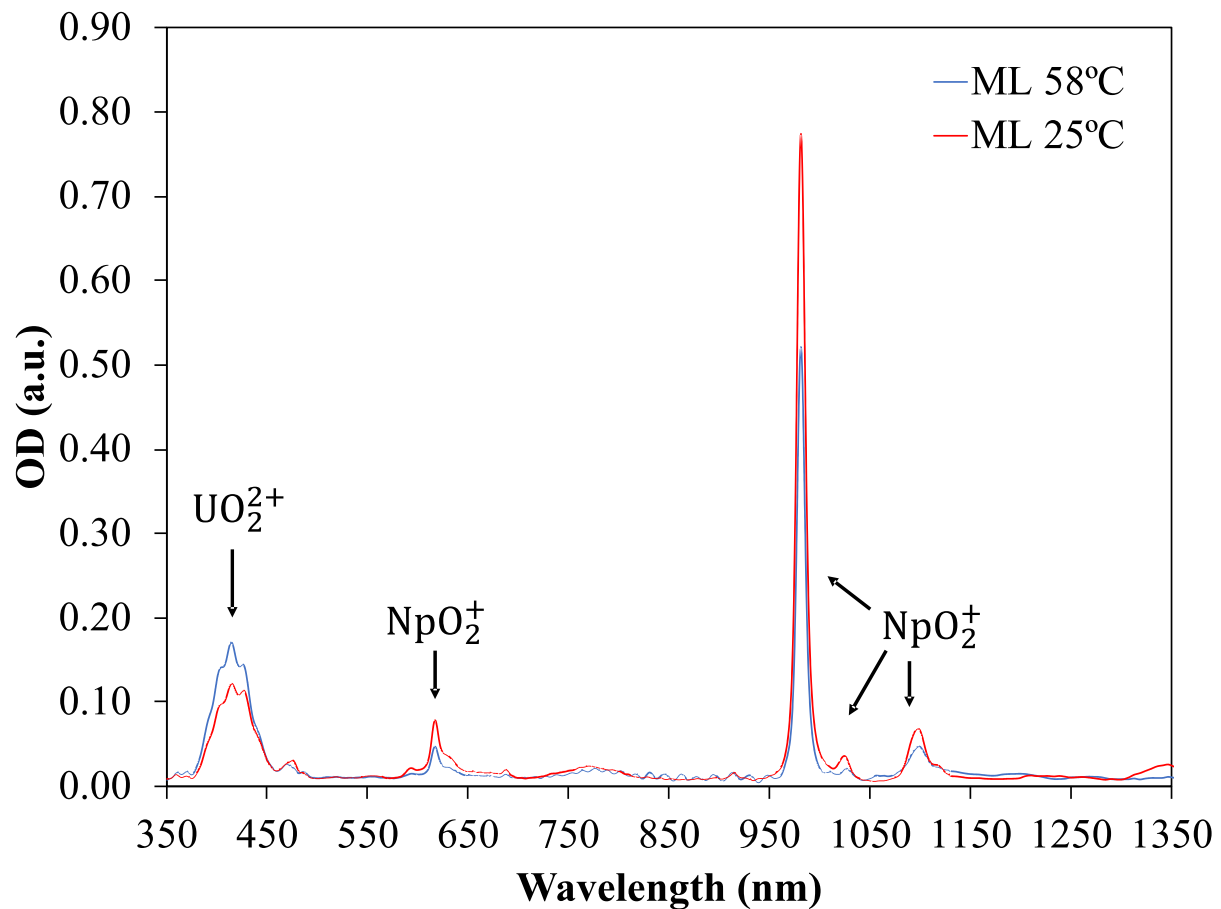


Fig. S7 Spectra of co-crystallization of UNH with  $\text{NpO}_2^+$  present before (blue) and after (red) crystallization diluted 100-fold.

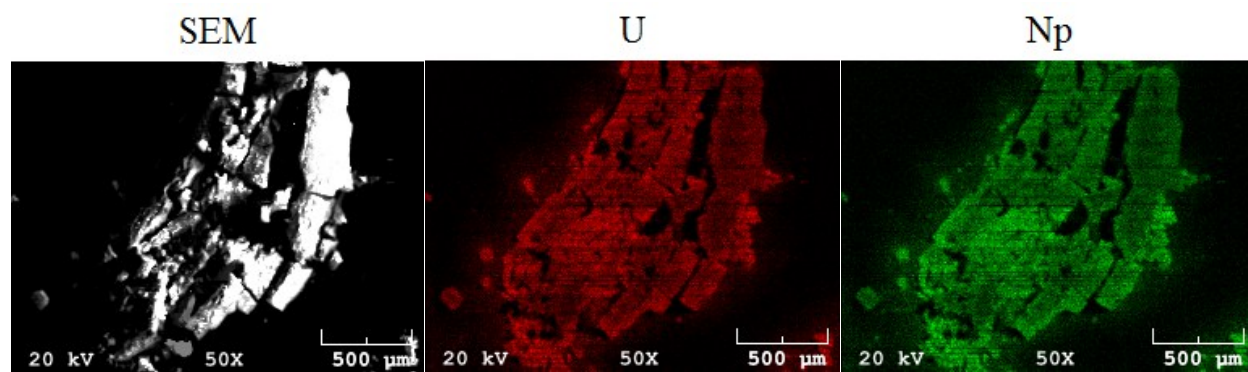


Fig. S8 SEM (left), EDS X-ray map of U (middle), and EDS X-ray map of Np (right) of crystallized UNH with  $\text{NpO}_2^{2+}$  incorporated.

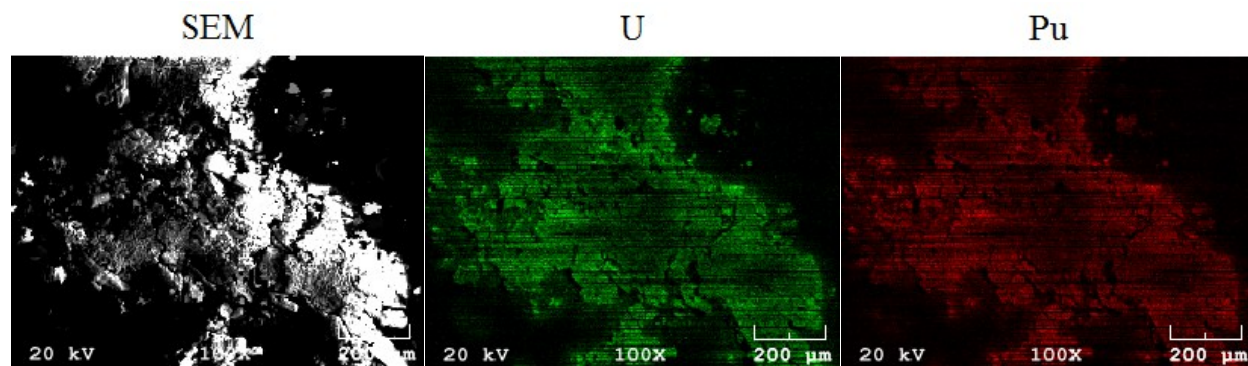


Fig. S9 SEM (left), EDS X-ray map of U (middle), and EDS X-ray map of Pu (right) of crystallized UNH with  $\text{PuO}_2^{2+}$  incorporated.

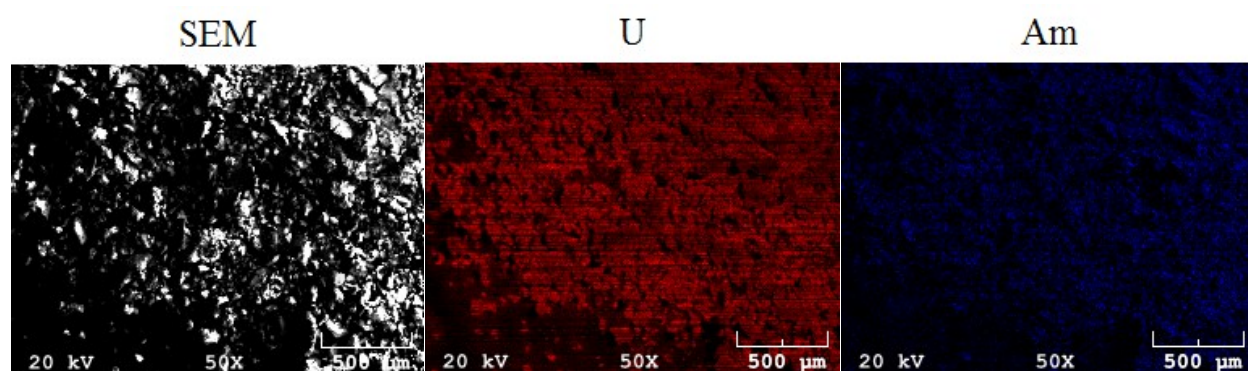


Fig. S10 SEM (left), EDS X-ray map of U (middle), and EDS X-ray map of Pu (right) of crystallized UNH with  $\text{AmO}_2^{2+}$  incorporated.

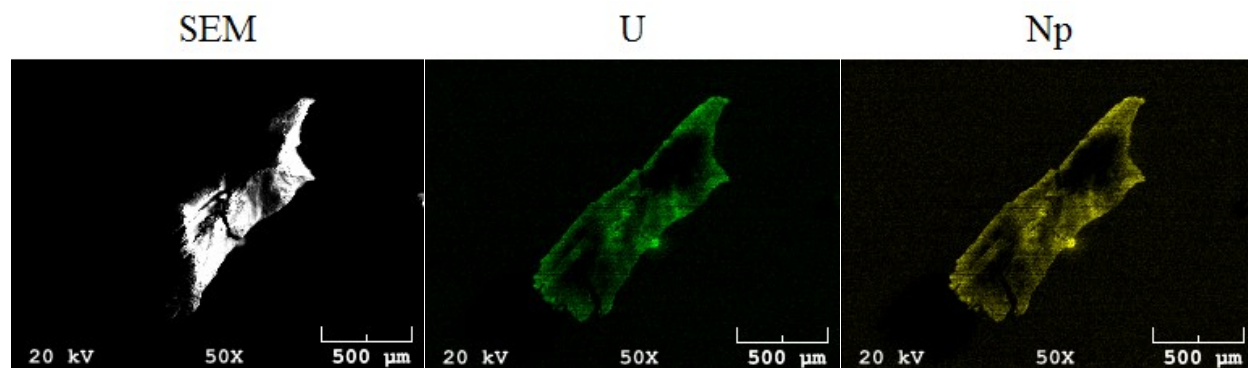


Fig. S11 SEM (left), EDS X-ray map of U (middle), and EDS X-ray map of Pu (right) of crystallized UNH with  $\text{NpO}_2^+$  incorporated.

## References:

- 1 E. Browne and R. B. Firestone, *Table of Radioactive Isotopes*, Wiley, New York, 1st edn., 1986.